Available online at www.sciencedirect.com
ScienceDirect
Journal of Magnetic Resonance 183 (2006) 160–165
JMR Journal of Magnetic Resonance
www.elsevier.com/locate/jmr

Communication

On the accurate measurement of amide one-bond ^{15}N–^{1}H couplings in proteins: Effects of cross-correlated relaxation, selective pulses and dynamic frequency shifts

Eva de Alba *, Nico Tjandra

Laboratory of Molecular Biophysics, National Heart, Lung, and Blood Institute, National Institutes of Health, 50 South Drive, Bethesda, MD 20892, USA

Received 29 June 2006; revised 10 August 2006
Available online 1 Septemeber 2006

Abstract

Amide one-bond ^{15}N–^{1}H scalar couplings of ^{15}N- and [^{15}N,^{2}H]-isotopically enriched ubiquitin have been measured with the Quantitative *J* approach by monitoring NMR signal intensity modulation. Scalar couplings of the non-deuterated protein are in average ~0.6 Hz larger than values of deuterated ubiquitin. This deviation is 30 times the error derived from experiment reproducibility. Refocusing dipole/dipole cross-correlated relaxation decreases the discrepancy to ~0.1 Hz, suggesting that it likely originates from relaxation interference. Alternatively, the subtraction of *J* values obtained at different magnetic fields largely reduces the relaxation effects. In contrast, the dynamic frequency shift whose main contribution to $^{1}J(^{15}N–^{1}H)$ arises from ^{15}N chemical shielding anisotropy/NH dipole cross-correlation, is not eliminated by refocusing spin evolution under this interaction. Furthermore, the average difference of $^{1}J(^{15}N–^{1}H)$ values at two magnetic fields closely agrees with the theoretical expected difference in the dynamic frequency shift.
Published by Elsevier Inc.

Keywords: NMR; Scalar couplings; Cross-correlated relaxation; Selective pulses; Dynamic frequency shifts

1. Introduction

The accurate measurement of one-bond ^{15}N–^{1}H scalar and dipolar couplings has become of great importance since the revolutionary application of residual dipolar couplings to the structural biology field [1–4]. As a result numerous NMR experiments aimed to measure both parameters have been designed in the last decade (see for example references [5–9]). Scalar and dipolar couplings are calculated either from resonance frequency splitting [10] or NMR signal intensity (Quantitative *J* approach [11]). Quantitative *J* experiments can be performed in two fashions; *J* values are obtained from the intensity ratio of signals originated from two spin operators that evolve with the coupling, or from the *J*-modulation of the intensity associated to a single operator.

Scalar couplings derived from frequency splitting are affected by inaccuracy in the determination of frequency values, which usually results from line broadening or partial signal intensity cancellation producing an artifact shift in the peak maximum.

In the Quantitative *J* approach where two operators are monitored, their different relaxation rates need to be accounted for to reduce measurement errors. In contrast, neither of these two sources of error affects Quantitative *J* methods based on the intensity modulation associated to a single operator.

J measurements can as well be affected by chemical shielding anisotropy/dipole (CSA/DD) and dipole/dipole (DD/DD) cross-correlated relaxation (CCR). In scalar couplings derived from frequency splitting, CCR modifies the peak shape leading to inaccuracy in frequency determination [12]. In contrast, signal intensity in Quantitative *J* experiments where either one or two spin operators are monitored, might be affected by magnetization transfer originated from CSA/DD and DD/DD CCR [6,13].

* Corresponding author. Fax: +1 301 402 3404.
E-mail address: dealbae@nhlbi.nih.gov (E.de Alba).

1090-7807/$ - see front matter Published by Elsevier Inc.
doi:10.1016/j.jmr.2006.08.003

Amide $^1J(^{15}N–^1H)$ couplings have been previously derived from the intensity ratio of signals associated to two spin operators [6]. The obtained values were found to vary by using a non-selective vs. a selective pulse used to suppress DD/DD cross-correlation. The discrepancies were attributed to processes of magnetization transfer that would differently modify the signal intensity associated to each operator. Cross-correlation interference has been theoretically analyzed and experimentally reported in protein $^1J(^{13}C–^1H)$ values measured by Quantitative J based on intensity modulation associated to a single operator [13]. This analysis indicates that J values are affected by CCR when the modification of intensity carries a change in the periodicity of the modulation. In contrast, any type of intensity modification would affect J values from Quantitative J based on the intensity ratio.

A different interfering mechanism of cross-correlated relaxation with coupling measurements is in the form of dynamic frequency shifts. The imaginary component of the spectral density function associated to CSA/DD cross-correlation induces a change in the scalar coupling commonly known as dynamic frequency shift [14]. For a two spin system, IS, the dynamic frequency shift (DFS) is described as [14,15]:

$$\begin{aligned}\mathrm{DFS}(I_{\mathrm{CSA}}/\mathrm{IS}_{\mathrm{DD}}) \approx {} & (1/10\pi)(\mu_0/4\pi)(h/2\pi) \\ & \times \sigma_{\mathrm{I}}\gamma_{\mathrm{I}}\gamma_{\mathrm{S}}(r_{\mathrm{I-S}})^{-3}(3\cos^2\theta - 1) \\ & \times 1/(1 + 1/(\omega_{\mathrm{I}}\tau_{\mathrm{c}})^2) \end{aligned} \quad (1)$$

where, τ_c is the overall correlation time of the protein, μ_0 is the susceptibility of the vacuum, h is the Planck's constant, γ_I and γ_S, are the gyromagnetic ratios of nuclei I and S, respectively, $r_{I–S}$ is the distance between nuclei I and S, θ is the angle between the principal axes of the CSA and DD interactions, σ_I is the parallel minus perpendicular components of the I CSA tensor, and ω_I is the angular Larmor frequency of I. Eq. (1) assumes that the motion is completely isotropic, the CSA tensor is axially symmetric and the effect of internal dynamics is not considered. It is noteworthy that under these conditions the absolute value of the DFS decreases at lower magnetic field strength. In the presence of CSA/DD CCR the dynamic frequency shift contributes to the measured J according to Eq. (1). Amide $^1J(^{15}N–^1H)$ couplings will be affected by the sum of two DFS values arising from CSA(^{15}N)/DD(NH) and CSA(^{1}H)/DD(NH) cross-correlated relaxation [14].

In addition to the previously mentioned interfering mechanisms, J couplings are affected by the difference in the relaxation rate of the in-phase and anti-phase spin operators resulting from scalar coupling [16]. As illustrated by Eq. (2), the larger the difference of the relaxation rates, the smaller the value of the apparent J [17].

$$J_{\mathrm{app}} = J - (\Delta R)^2/[(2\pi)^2(2J)] \quad (2)$$

where, J_{app} is the apparent scalar coupling constant, J is the coupling constant in the absence of differential relaxation and ΔR is the difference between the transverse relaxation rates of the in-phase and anti-phase operators.

For large coupling constants such as protein $^1J(^1H–^{13}C)$ (~140 Hz) and amide $^1J(^1H–^{15}N)$ (~−94 Hz), the operators will interconvert fast during the J evolution period, averaging their relaxation rates [18], and therefore, decreasing the influence of this relaxation effect in the J value [17].

Aiming to obtain accurate amide one-bond $^{15}N–^1H$ couplings in proteins, it is the purpose of this communication to analyze several factors affecting their measurement. We report herein the magnitude of relaxation interference when using the Quantitative J approach based on a single operator, and evaluate the efficiency of selective pulses to cancel relaxation effects. Our data suggest that the interference arising from DD/DD cross-correlation is almost eliminated by refocusing spin evolution under this interaction or by subtracting data obtained at two magnetic fields. In contrast, the dynamic frequency shift does not vanish when CSA/DD CCR is refocused. Additionally, the comparison of J values obtained at different magnetic fields indicates that the DFS originated from CSA(^{15}N)/DD(NH) is positive.

2. Results and discussion

The NMR experiments used to obtain one-bond $^{15}N–^1H$ scalar couplings of the protein ubiquitin are shown in Fig. 1. In the pulse scheme of Fig. 1a [5] transverse ^{15}N magnetization anti-phase with respect to ^1H ($2N_yH_z^N$) is created at point a, and evolves with the scalar coupling (J) during 2λ as follows:

$$2\mathrm{N}_y\mathrm{H}_z^N\cos(\pi J 2\lambda) - \mathrm{N}_x\sin(\pi J 2\lambda) \quad (3)$$

After ^{15}N chemical shift evolution during t_1, the collected operator $2N_yH_z^N$, is a function of the $^{15}N–^1H$ scalar coupling and the resulting signal intensity can be described as:

$$I = (A_0\cos(\pi J 2\lambda) + A_1)\exp(-A_2 2\lambda) \quad (4)$$

where A_0 is the intensity of a reference signal (e.g. 1st time point) and A_1 represents the amount of magnetization that does not evolve with J because of imperfections in the π pulses. The exponential function, $\exp(-A_2 2\lambda)$ accounts for signal intensity decay due to relaxation pathways and evolution with coupling to passive spins. A Gaussian function is commonly used to take into account intensity decay resulting from passive coupling [19]. We found J differences of less than 0.01 Hz by including this function into Eq. (4) (smaller than the experimental error, 0.02 Hz), indicating that the exponential function suffices to account for passive coupling.

A total of 15 experiments are acquired in which the value of λ is modified such that the modulated function is sampled at three zero crossings (Fig. 2). J values are derived from the fitting to Eq. (4) of peak intensities in the 15 [$^1H–^{15}N$]-HSQC spectra as a function of 2λ.

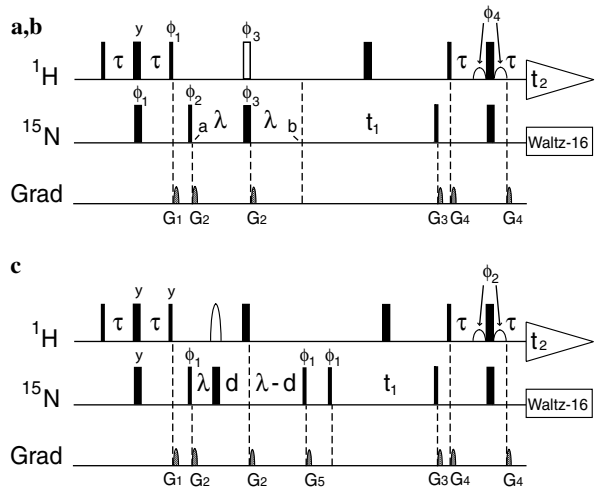

Fig. 1. NMR pulse schemes for $^1J(^{15}\mathrm{N}–\mathrm{H}^N)$-modulated [^{1}H–^{15}N]-HSQC, (a) with effective DD/DD cross-correlated relaxation, (b) where DD/DD cross-correlated relaxation is refocused, (c) with effective CSA(^{15}N)/DD(NH) cross-correlated relaxation. Narrow and wide bars correspond to 90° and 180° flip angles. Small white bell shapes are 90° ^{1}H pulses (~1 ms) included in the WATERGATE module for water suppression [25]. The white bar indicates (a) 180° hard pulse, (b) REBURP pulse [20] for selective H^N inversion (1.4 ms at 600 MHz and 2.33 ms at 360 MHz, for 4.5 ppm inversion bandwidth). The large white bell shape in (c) is a REBURP pulse [20] for selective H^α and H^β inversion (1.11 ms at 600 MHz and 1.85 ms at 360 MHz, for 5.85 ppm inversion bandwidth). Unless otherwise indicated phases of radiofrequency pulses are applied on x. For (a) and (b) $\phi_1 = 8(y), 8(-y)$; $\phi_2 = x, -x$; $\phi_3 = 2(x), 2(y), 2(-x), 2(-y)$; $\phi_4 = -x$; receiver $= x, 2(-x), 2(x), 2(-x), x, -x, 2(x), 2(-x), 2(x), -x$. For (c) $\phi_1 = x, -x$; $\phi_2 = -x$; receiver $= x, -x$. The applied time delays are as follows; $\tau = 2.25$ ms. For (a) $\lambda_a = 19.1, 19.5, 19.8, 20.7, 21.2, 24.2, 24.6, 25.1, 26.2, 26.5, 29.9, 30.3, 30.7, 31.1$, and 31.9 ms. Assuming that the 180° ^{15}N and ^{1}H pulses are applied simultaneously and that $\tau_{180}(\mathrm{N}) \gg \tau_{180}(\mathrm{H})$, the fraction $2/\pi$ of $\tau_{180}(\mathrm{N})$ needs to be added to 2λ to account for J evolution during pulses of finite length in order to extract J values from signal modulation [5,26]. For (b) $\lambda_b = \lambda_a - [\tau_{\mathrm{REBURP}}/2 - \tau_{90}(\mathrm{N})]$. λ_b values are shorter than λ_a such that the time during which the magnetization is in the transverse plane is identical in experiments (a) and (b). J evolution is assumed to be active during the duration of the REBURP pulse. Therefore, the length of this pulse is added to 2λ, in analogy to previously reported experiments for ^1J(C–H) measurements in which the total length of the 180° pulse affecting the spin in the longitudinal axis is added to the J evolution time [27]. For (c) $d = 10$ ms, $\lambda_c = \lambda_a - [\tau_{\mathrm{REBURP}}/2 - \tau_{90}(\mathrm{N})]$. Analogously to experiments (a) and (b), the time $\tau_{180}(\mathrm{H})$ and the fraction $4/\pi$ of $\tau_{90}(\mathrm{N})$ need to be added to $2(\lambda - d)$ to take into account J evolution during these pulses. Quadrature detection in the t_1 dimension is obtained using the States-TPPI protocol [28], by simultaneously incrementing ϕ_2 and ϕ_3 in (a) and (b) and ϕ_1 in (c). For the three pulse schemes, pulse field gradients have a sine-bell shape with amplitude of 25 G/cm at their center. Gradient durations are: $G_{1,2,3,4,5} = 5.0$, 2.3, 1.0, 0.4, and 2.0 ms. ^{15}N decoupling during ^{1}H acquisition was achieved by applying the WALTZ-16 decoupling sequence [29]. NMR experiments were performed at 360 and 600 MHz at 27 °C.

In the experiment of Fig. 1a, amide ^{15}N is coupled to protons that are two or three bonds away, such as H^α and H^β. Considering ^{15}N coupling to a second ^{1}H in addition to H^N, the magnetization at point b can be described as:

$$\begin{aligned} &2\mathrm{N}_y\mathrm{H}_z^N \cos(\pi J 2\lambda)\cos(\pi J_j 2\lambda) - \mathrm{N}_x \sin(\pi J 2\lambda)\cos(\pi J_j 2\lambda) \\ &\quad - 2\mathrm{N}_y\mathrm{H}_z^j \sin(\pi J 2\lambda)\sin(\pi J_j 2\lambda) \\ &\quad - 4\mathrm{N}_x\mathrm{H}_z^N\mathrm{H}_z^j \cos(\pi J 2\lambda)\sin(\pi J_j 2\lambda) \end{aligned} \quad (5)$$

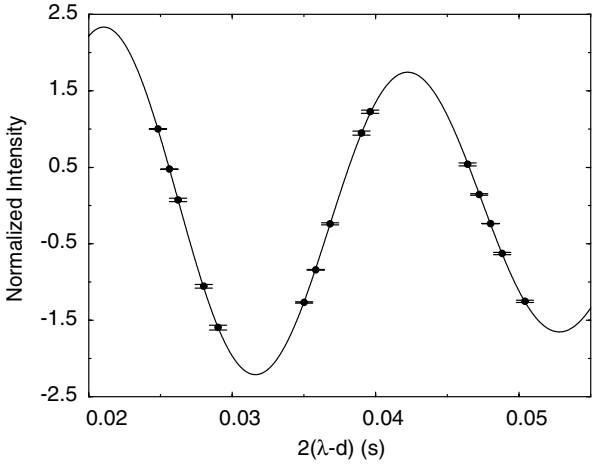

Fig. 2. Fitting to Eq. (7) of normalized experimental intensity modulated with time for the $^{15}\mathrm{N}–\mathrm{H}^N$ amide group of ubiquitin Leu 56 using the pulse scheme of Fig. 1c at 600 MHz. Error bars correspond to normalized errors calculated from reproducibility.

where, J is the amide one-bond $^{15}\mathrm{N}–\mathrm{H}^N$ coupling and J_j is the scalar coupling between amide ^{15}N and H^α or H^β. In the experiment of Fig. 1a, magnetization evolution with both CSA(^{15}N)/DD(NH) and CSA(^{1}H)/DD(NH) cross-correlated relaxation is refocused. In contrast, magnetization evolves during 2λ with DD/DD cross-correlated relaxation. This interaction can involve the $^{15}\mathrm{N}–\mathrm{H}^N$ dipole, and a dipole between the amide ^{15}N and a second ^{1}H scalar coupled to it, for example H^α or H^β.

As a result of this interaction magnetization is transferred between the operators, $2\mathrm{N}_y\mathrm{H}_z^N$ and $2\mathrm{N}_y\mathrm{H}_z^j$. At point b (Fig. 1a), the evolution of the collected operator can be described as:

$$\begin{aligned} &2\mathrm{N}_y\mathrm{H}_z^N[\cos(\pi J 2\lambda)\cos(\pi J_j 2\lambda)\cosh(\Gamma 2\lambda) + \sin(\pi J 2\lambda) \\ &\quad \times \sin(\pi J_j 2\lambda)\sinh(\Gamma 2\lambda)] \end{aligned} \quad (6)$$

where Γ is the cross-correlated relaxation rate between the amide $^{15}\mathrm{N}–\mathrm{H}^N$ dipole and the amide $^{15}\mathrm{N}–\mathrm{H}^{\alpha/\beta}$ dipole.

Magnetization transfer between the operators, $2\mathrm{N}_y\mathrm{H}_z^N$ and $2\mathrm{N}_y\mathrm{H}_z^j$ can result as well from $^1\mathrm{H}–^1\mathrm{H}$ cross-relaxation (Nuclear Overhauser Effect). The modification of signal intensity arising from this relaxation pathway is not expected to change the J value since the periodicity of the modulation will not be affected.

Experiments in Fig. 1a and b are identical, except for the application of a REBURP pulse [20] to selectively invert $^1\mathrm{H}^N$. This pulse refocuses magnetization evolution with DD/DD cross-correlated relaxation and scalar coupling of amide ^{15}N to any other ^{1}H different from $^1\mathrm{H}^N$. In the experiment of Fig. 1b, evolution with CSA(^{15}N)/DD(NH) and CSA(^{1}H)/DD(NH) cross-correlated relaxation is as well refocused.

Fig. 3a shows that $J(^{15}\mathrm{N}–\mathrm{H}^N)$ values obtained with the experiment of Fig. 1a for ^{15}N-labeled ubiquitin are in average 0.6 Hz larger than those of [^{15}N,^{2}H]-enriched ubiquitin. This systematic deviation, which is 30 times larger than the

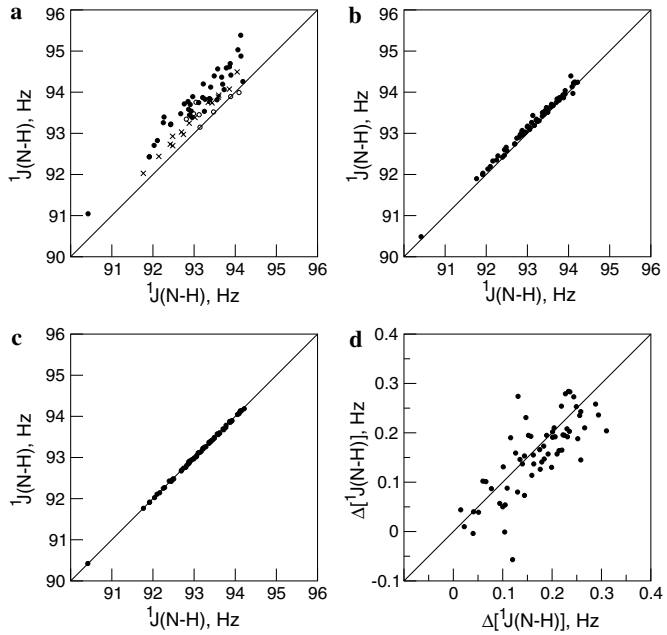

Fig. 3. (a) $^1J(^{15}N–H^N)$ values at 600 MHz obtained with the experiment of Fig. 1a for deuterated (x axis) and non-deuterated (y axis) ubiquitin. Black circles, crosses and open circles correspond to residues with two beta protons, one beta proton, Gly and highly flexible residues, respectively. (b) $^1J(^{15}N–H^N)$ data obtained at 600 MHz with the pulse scheme of Fig. 1b for deuterated (x axis) non-deuterated (y axis) ubiquitin. (c) $^1J(^{15}N–H^N)$ values at 600 MHz for [^{15}N,^{2}H]-labeled ubiquitin obtained with the experiment of Fig. 1b (x axis) and Fig. 1a (y axis). (d) Difference in $^1J(^{15}N–H^N)$ values at 360 and 600 MHz for non-deuterated ubiquitin measured with the pulse scheme of Fig. 1b (x axis) and Fig. 1a (y axis). Residues with low intensity because of exchange processes (Glu 24, Gly 53) and residues that are partially overlapped (Asp 21, Ala 28, Leu 69, Leu 73) are not represented. Ile 36 is excluded because its $^1H^N$ chemical shift is close to the edge of the selective pulse excitation profile. ^{15}N-labeled ubiquitin was expressed and purified as previously described [30]. [^{15}N,^{2}H]-labeled ubiquitin was purchased from Spectra Stable Isotopes.

experimental error derived from reproducibility (0.02 Hz), points out the interference of relaxation with scalar coupling measurements. The discrepancy is more pronounced for residues containing two vs. one beta proton, as shown in Fig. 3a. The systematic deviation can result from a more complex magnetization evolution with J than that described in Eq. (3). Processes of magnetization transfer resulting from DD/DD cross-correlation as defined in Eq. (6) will modify the periodicity of the signal modulation, thus affecting the obtained J value [13]. It is possible to theoretically estimate the expected cross-correlation interference, as previously described for $^1J(^{13}C–^1H)$ measurements [13]. Signal intensity has been simulated considering magnetization evolution with an ideal $J(^{15}N–H^N) = -94$ Hz, and three DD/DD CCR pathways, i.e. $N_i–H^N/N_i–H^\alpha_{i-1}$, $N_i–H^N/N_i–H^\alpha_i$, $N_i–H^N/N_i–H^\beta_i$. By using Eq. (4) to fit the simulated intensity the obtained $J(^{15}N–H^N) = -94.16$ Hz. The deviation 0.16 Hz closely agrees with the average discrepancy of residues with one beta proton, 0.2 Hz (Fig. 3a). The larger differences shown in Fig. 3a for residues with two beta protons probably arise from more complicated relaxation mechanisms that have not been accounted for.

The mentioned DD/DD CCR pathways are absent in ^{2}H-labeled ubiquitin. Therefore, should the interference prove valid, non-deuterated ubiquitin J values obtained with the pulse scheme of Fig. 1b will become similar to those of deuterated ubiquitin, and the later will not be affected by the application of a selective vs. a non-selective pulse. As shown in Fig. 3b $J(^{15}N–H^N)$ values of non-deuterated ubiquitin decrease by the application of the selective pulse, while J values of deuterated ubiquitin do not show a systematic deviation and are unmodified within the experimental error (Fig. 3c). The discrepancy is almost completely counter-balanced by selective pulse application. Nevertheless a small deviation of ~0.1 Hz is observed (Fig. 3b). To test if this small difference results from magnetization evolution with cross-correlation during the relatively long selective pulse, we calculated the differences between non-deuterated and deuterated ubiquitin J values obtained at two magnetic fields (600 and 360 MHz) with the pulse scheme of Fig. 1b. To achieve the same inversion bandwidth (4.5 ppm) the length of the selective pulse used at the two magnetic fields is substantially different (1.4 ms at 600 MHz vs. 2.33 ms at 360 MHz). The obtained data are very similar within the experimental error (data not shown), suggesting that the observed difference does not result from residual CCR during the selective pulse. Differential relaxation of the in-phase and anti-phase operators as illustrated in Eq. (2) does not explain the observed discrepancy. The absolute J values of non-deuterated ubiquitin should be smaller than those of deuterated ubiquitin according to this effect, since a larger difference in the relaxation rate of the operators is expected for non-deuterated ubiquitin [16]. In contrast, the opposite result is experimentally obtained (Fig. 3b). Incomplete refocusing of several DD/DD CCR pathways could explain the discrepancy.

Differences in $J(^{15}N–H^N)$ couplings measured at two magnetic fields can be used to estimate the dipolar and DFS contributions [5], therefore, it is interesting to know if relaxation effects can be eliminated by subtraction. Fig. 3d shows that DD/DD CCR effects are largely reduced by subtracting J values at two magnetic fields, suggesting that magnetic field strength does not significantly affect the interference.

The pulse sequence of Fig. 1c was designed to evaluate the dynamic frequency shift contribution to scalar coupling measurements. In this experiment, ^{15}N magnetization is transverse during the same amount of time as in the pulse sequence of Fig. 1a to avoid differential relaxation effects between experiments. In contrast $^{15}N–H^N$ scalar coupling evolves during $2(\lambda - d)$, thus signal intensity is modulated according to the following equation:

$$I = (A_0 \cos[\pi J 2(\lambda - d)] + A_1) \exp(-A_2 2\lambda) \quad (7)$$

Parameters A_0, A_1 and A_2 are defined in Eq. (4).

In the experiment of Fig. 1c, magnetization evolution with CSA(^{1}H)/DD(NH) is refocused, on the contrary, CSA(^{15}N)/DD(NH) CCR is effective during 2d.

N_x magnetization created by scalar coupling evolution (Eq. (3)) can be transferred to $2N_xH_z^N$ as a result of effective CSA(^{15}N)/DD(NH) cross-correlation. $2N_xH_z^N$ magnetization will evolve with ^{15}N chemical shift during t_1 into $2N_yH_z^N$ (Fig. 1c), which will be sine modulated. After Fourier transformation dispersive signals might be generated since the original $2N_yH_z^N$ term resulting from scalar coupling (Eq. (3)) will be cosine modulated with chemical shift. To suppress this artifact by eliminating N_x magnetization right before the t_1 module, two 90° ^{15}N pulses sandwiching a pulse field gradient were incorporated in the experiment of Fig. 1c. Although this pulse scheme has been applied to [^{15}N,^{2}H]-labeled ubiquitin, residual DD/DD cross-correlation might arise from incomplete ^{2}H-labeling (~3%). Therefore, a REBURP pulse [20] that selectively inverts H^α and H^β spins was applied to refocus spin evolution under this interaction. By comparing J values obtained with the experiments of Fig. 1a, where CSA/DD cross-correlation evolution is refocused, and Fig. 1c, it could be possible to measure the dynamic frequency shift associated to the CSA(^{15}N)/DD(NH) interaction.

The theoretical DFS value originated from CSA(^{15}N)/DD(NH) cross-correlated relaxation should be positive, according to previously reported equations ([14,15], Eq. (1)) if isotropic motion and almost collinear interactions are assumed, and considering that the ^{15}N CSA tensor is nearly axially symmetric [21]. The former conditions are probably satisfied by the nearly isotropic diffusion of ubiquitin and an angle (θ) between the N–H bond-vector and the unique principal axis of the ^{15}N CSA tensor ranging from 0° to 25° [22]. The expected average value of the DFS in ubiquitin is 0.42 Hz at 600 MHz and 0.27 Hz at 360 MHz using the following parameters; correlation time $\tau_c = 4.04$ ns at 27 °C [23], σ (^{15}N) ~ −172 ppm, $\theta \sim 24°$ [22], $r_{N-H} = 1.02$ Å, and $\gamma_N < 0$. In contrast, the DFS value arising from CSA(^{1}H)/DD(NH) can be considered constant at the two magnetic fields since in the slow motion limit $\omega_H \tau_c \gg 1$ (Eq. (1)).

Although Quantitative J methods do not provide the sign of the scalar coupling, it is well known that $J(^{15}N–H^N) < 0$. Therefore, the contribution of a positive DFS to a negative scalar coupling results in the decrease of its absolute value measured by Quantitative J. Furthermore, in the absence of other effects, $J(^{15}N–H^N)$ absolute values obtained with this approach are expected to be larger the lower the applied magnetic field, since the DFS contribution decreases. Thus, absolute J values measured with the experiment of Fig. 1c should be smaller than those provided by the pulse scheme in Fig. 1a. The data obtained from both experiments are very similar (Fig. 4a), suggesting that the dynamic frequency shift is not eliminated even when spin evolution under this interaction is refocused. In contrast, it has been previously reported that CSA/DD cross-correlation can be cancelled in Hartmann–Hahn selective coherence transfer experiments, vanishing the DFS contribution [24]. The effect of the DFS is shown in Fig. 4b, where absolute $J(^{15}N–H^N)$ values obtained at 360 and 600 MHz are compared. When considering the negative sign of $J(^{15}N–H^N)$, the average difference between the data at 360 and 600 MHz is ~−0.15 Hz, as expected from the decrease in the positive value of DFS at the lower magnetic field. This result agrees with the theoretical expected difference of the average dynamic frequency shift at the two magnetic fields (~−0.15 Hz). Previously reported calculations indicate that the DFS arising from the CSA(^{15}N)/DD(NH) interaction is negative, provided that motion is isotropic and the interactions are close to collinear [5,15]. Experimentally, the change in sign of this theoretical result can be easily overlooked if the negative value of $J(^{15}N–H^N)$ is not taken into account [5]. Our experimental results show that, under the mentioned conditions, the dependence of the negative $J(^{15}N–H^N)$ values with the magnetic field strength can only be explained if the DFS associated to CSA(^{15}N)/DD(NH) CCR is positive.

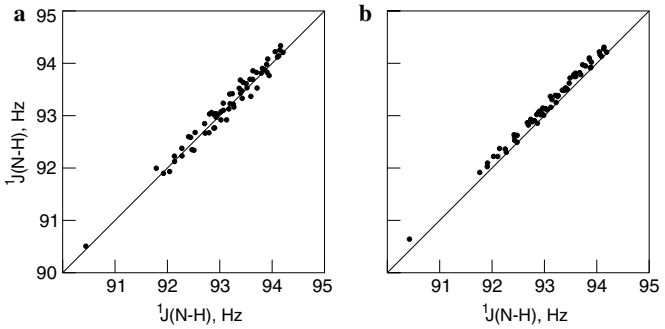

Fig. 4. (a) $^1J(^{15}N–H^N)$ values at 600 MHz obtained with the pulse scheme of Fig. 1a (x axis), where the two 90° ^{15}N pulses flanking a pulse field gradient were added to emulate pulse scheme of Fig. 1c. $^1J(^{15}N–H^N)$ values at 600 MHz obtained with the experiment of Fig. 1c (y axis). (b) $^1J(^{15}N–H^N)$ values of [^{15}N,^{2}H]-labeled ubiquitin obtained at 600 MHz (x axis) and 360 MHz (y axis) with the experiment of Fig. 1a.

3. Conclusions

By comparing $J(^{15}N–H^N)$ values of non-deuterated and deuterated ubiquitin we show the magnitude of magnetization relaxation effects on scalar coupling measurements. This interference results from DD/DD cross-correlated relaxation and is almost completely eliminated by applying a selective pulse to refocus spin evolution under this interaction. Additionally, relaxation effects can be greatly reduced by subtracting couplings obtained at two magnetic fields. In contrast, the dynamic frequency shift cannot be eliminated when CSA/DD cross-correlation is refocused. In ubiquitin, the comparison of average $J(^{15}N–H^N)$ values obtained at two magnetic fields to the theoretical dynamic frequency shift difference indicates that the DFS contribution is positive.

Acknowledgments

The authors thank Professor Lawrence G. Werbelow for useful comments on dynamic frequency shifts. This work was supported by the Intramural Research Program of the NIH, National Heart, Lung, and Blood Institute.

References

[1] J.H. Prestegard, H.M. Al-Hashimi, J.R. Tolman, NMR structures of biomolecules using field oriented media and residual dipolar couplings, Q. Rev. Biophys. 33 (2000) 371–424.
[2] E. de Alba, N. Tjandra, NMR dipolar couplings for the structure determination of biopolymers in solution, Prog. NMR Spectrosc. 40 (2002) 175–197.
[3] J.H. Prestegard, K.L. Mayer, H. Valafar, G.C. Benison, Determination of protein backbone structures from residual dipolar couplings, Meth. Enzymol. 394 (2005) 175–209.
[4] A. Bax, A. Grishaev, Week alignment NMR: a hawk-eyed view of biomolecular structure, Curr. Opin. Struct. Biol. 15 (2005) 563–570.
[5] N. Tjandra, S. Grzesiek, A. Bax, Magnetic field dependence of nitrogen-proton J splittings in ^{15}N-enriched human ubiquitin resulting from relaxation interference and residual dipolar coupling, J. Am. Chem. Soc. 118 (1996) 6264–6272.
[6] J.R. Tolman, J.H. Prestegard, A quantitative J-correlation experiment for the accurate measurement of one-bond amide ^{15}N–^{1}H couplings in proteins, J. Magn. Reson. 112 (1996) 245–252.
[7] M. Ottiger, F. Delaglio, A. Bax, Measurement of J and dipolar couplings from simplified two-dimensional NMR spectra, J. Magn. Reson. 131 (1998) 373–378.
[8] M.H. Lerche, A. Meissner, F.M. Poulsen, O.W. Sörensen, Pulse sequences for the measurement of one-bond ^{15}N–^{1}H coupling constants in the protein backbone, J. Magn. Reson. 140 (1999) 259–263.
[9] R.L. McFeeters, C.A. Fowler, V.V. Gaponenko, R.A. Byrd, Efficient and precise measurement of H^{α}–C^{α}, C^{α}–C', C^{α}–C^{β} and H^{N}–N residual dipolar couplings from 2D H^{N}–N correlation spectra, J. Biomol. NMR 31 (2005) 35–47.
[10] C. Griesinger, O.W. Sörensen, R.R. Ernst, Correlation of connected transitions by two-dimensional NMR spectroscopy, J. Chem. Phys. 85 (1986) 6837–6843.
[11] A. Bax, G.W. Vuister, S. Grzesiek, F. Delaglio, A.C. Wang, R. Tschudin, G. Zhu, Measurement of homo- and heteronuclear J couplings from Quantitative J correlation, Meth. Enzymol. 239 (1994) 79–105.
[12] N. Tjandra, A. Bax, Measurement of dipolar contributions to $^{1}J_{CH}$ splittings from magnetic-field dependence of J modulation in two-dimensional NMR spectra, J. Magn. Reson. 124 (1997) 512–515.
[13] E. de Alba, N. Tjandra, Interference between cross-correlated relaxation and the measurement of scalar and dipolar couplings by Quantitative J, J. Biomol. NMR 35 (2006) 1–16.
[14] L.G. Werbelow, The dynamic frequency shift, in: D.M. Grant, R.K. Harris (Eds.), The Encyclopedia of Nuclear Magnetic Resonance, vol. 6, Wiley, London, 1996, pp. 4072–4078.
[15] R. Brüschweiler, Cross-correlation-induced J coupling, Chem. Phys. Lett. 257 (1996) 119–122.
[16] G.S. Harbison, Interference between J-couplings and cross-relaxation in solution NMR spectroscopy: consequences for macromolecular structure determination, J. Am. Chem. Soc. 115 (1993) 3026–3027.
[17] A. Rexroth, P. Schmidt, S. Szalma, T. Geppert, H. Schwalbe, C. Griesinger, New principle for the determination of coupling constants that largely suppresses differential relaxation effects, J. Am. Chem. Soc. 117 (1995) 10389–10390.
[18] R. Ghose, J.H. Prestegard, Improved estimation of CSA-dipolar coupling cross-correlation rates from laboratory-frame relaxation experiments, J. Magn. Reson. 134 (1998) 308–314.
[19] M. Ottiger, F. Delaglio, J.L. Marquardt, N. Tjandra, A. Bax, Measurement of dipolar couplings for methylene and methyl sites in weakly oriented macromolecules and their use in structure determination, J. Magn. Reson. 134 (1998) 365–369.
[20] H. Geen, R. Freeman, Band-selective radiofrequency pulses, J. Magn. Reson. 93 (1991) 93–141.
[21] G. Cornilescu, A. Bax, Measurement of proton, nitrogen, and carbonyl chemical shielding anisotropies in a protein dissolved in a dilute liquid crystalline phase, J. Am. Chem. Soc. 122 (2000) 10143–10154.
[22] D. Fushman, N. Tjandra, D. Cowburn, Direct measurement of ^{15}N chemical shift anisotropy in solution, J. Am. Chem. Soc. 120 (1998) 10947–10952.
[23] S-L. Chang, N. Tjandra, Temperature dependence of protein backbone motion from carbonyl ^{13}C and amide ^{15}N NMR relaxation, J. Magn. Reson. 174 (2005) 43–53.
[24] H. Desvaux, R. Kümmerle, J. Kowalewski, C. Luchinat, I. Bertini, Direct measurement of dynamic frequency shift induced by cross-correlations in ^{15}N-enriched proteins, Chemphyschem. 4 (2004) 959–965.
[25] M. Piotto, V. Saudek, V. Sklenar, Gradient-tailored excitation for single-quantum NMR spectroscopy of aqueous solutions, J. Biomol. NMR 2 (1992) 661–665.
[26] R.R. Ernst, G. Bodenhausen, A. Wokaun, Principles of Nuclear Magnetic Resonance in one and two dimensions in: J.S. Rowlinson (Ed.), Claredon Press, Oxford, 1989, p. 123.
[27] G.W. Vuister, F. Delaglio, A. Bax, The use of $^{1}J_{C\alpha H\alpha}$ coupling constants as a probe for protein backbone conformation, J. Biomol. NMR 3 (1993) 67–80.
[28] D. Marion, M. Ikura, R. Tschudin, A. Bax, Rapid recording of 2D NMR spectra without phase-cycling. Application to the study of hydrogen exchange in proteins, J. Magn. Reson. 85 (1989) 393–399.
[29] A.J. Shaka, J. Keeler, T. Frenkiel, R. Freeman, An improved sequence for broadband decoupling: WALTZ-16, J. Magn. Reson. 52 (1983) 335–338.
[30] G.A. Lazar, J.R. Desjarlais, T.M. Handel, De novo design of the hydrophobic core of ubiquitin, Prot. Sci. 6 (1997) 1167–1178.